

## Aggregate behaviour in concrete materials under high temperature conditions

G. Mazzucco<sup>1</sup>, C.E. Majorana<sup>1</sup>, V.A. Salomoni<sup>1</sup> and G. Xotta<sup>2</sup>

<sup>1</sup>*Department of Civil, Environmental and Architectural Engineering (DICEA), University of Padova, Via F. Marzolo 9, 35131 Padova, Italy*

<sup>2</sup>*Department of Civil and Environmental Engineering, Cullen College of Engineering, University of Houston, N107 Engineering Building 1, Houston – TX 77204-4003, USA*

**Abstract.** The effect of aggregates characterized by different porosities is here investigated, in order to catch the damage scenarios related to the various inclusions types and hence to understand the role of aggregates porosity on spalling when concrete is exposed to fire. For this purpose, the 3D fully coupled thermo-hydro-mechanical finite element code NEWCON3D has been adopted, able to characterize concrete behaviour at the meso scale level under high temperature regimes.

### 1. INTRODUCTION

Concrete has a highly heterogeneous microstructure and its composite behaviour is exceedingly complex. For obtaining a deeper understanding, theoretical studies based on micromechanics analysis of the interaction between various components of concrete have been developed for deducing the macroscopic constitutive behaviour of concrete. However, the microstructure and properties of the individual components of concrete and their effects on the macroscopic material behaviour have not been generally taken into account. For such details to be included into the computational analysis, concrete needs to be analysed as a multi-scale composite material where the microstructure is realistically simulated.

Specifically, as for the level of observation lower than the macroscopic one, i.e. the meso scale, it provides a more realistic description of concrete at the macro scale, influenced by the geometry and the properties of its components. Moreover a thorough knowledge of concrete at the meso-scale level is nowadays essential for a better understanding of specific phenomena in concrete, especially those where aggregate content and their thermal properties have a crucial role, e.g. spalling.

Spalling corresponds to the separation of pieces of concrete from the surface of a structural element when it is exposed to high and rapidly rising temperatures. It is stochastic in nature; in fact for specimens from the same batch, and under identical conditions, some could spall while others do not. Many information on this phenomenon, particularly on explosive spalling, have been obtained after damage caused by the fire in the tunnels, such as the Danish Great Belt one, the Channel Tunnel, Mont Blanc and Tauern tunnels.

In this paper the effect of aggregates characterized by different porosities is investigated, in order to catch the damage scenarios related to the different inclusions types and hence to understand the role of aggregates porosity on spalling when concrete is exposed to fire. For this purpose, the 3D fully coupled thermo-hydro-mechanical finite element code NEWCON3D [1] has been adopted, able to characterize concrete behaviour at the meso scale level under different temperature regimes [2]. Particularly, it is

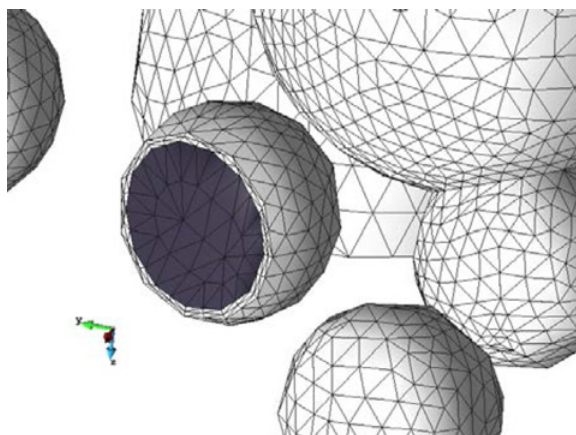


**Figure 1.** Three dimensional ITZ representation in the numerical models.

assumed that creep of concrete obeys to the B3 model proposed by Bažant and Baweja [3], instead damage obeys to the Mazars' damage law [4] with non-local correction.

## 2. ITZ FORMATION AND CHARACTERIZATION

Cement grains size ranges from less than a micron up to 100 microns, while the aggregates are several orders of magnitude larger. This difference of size means that the aggregate particle is an obstacle which disrupts the packing of cement grains, resulting in the so called “wall effect” [5]. The origin of the ITZ lies in this “wall effect” of packing against the relatively flat aggregate surface.

The low porosity which characterizes the aggregates during the hydration process causes an accumulation of water around the grains and a consequent water/cement ratio increase in this zone, thus decreasing concrete performances.

In these layers, between the cement paste and the aggregates, the high w/c ratio increases concrete porosity (often about two or three times more than the cement paste) and the ITZ strength is lower than the average concrete strength. Generally the ITZ is represented as a layer with a constant thickness around the grains (the thickness is assumed as a fraction of the aggregate dimension, about 1/10 of the aggregate diameter) even if the water stagnation depends on gravitational effects, and the ITZ thickness results greater in the lower face of the grains. The evaluation of the real thickness of the ITZ around the aggregates is extremely complicated and is dependent on the aggregates shape, the initial porosity and the w/c ratio. For this reasons in this study the ITZ thickness has been considered approximately constant around the grains with an average thickness (see Figure 1).

The thickness of the ITZ is quite small, between 10 and 50  $\mu\text{m}$ , and its mechanical characterization is not easily reachable but, as a first approximation, the elastic and shear modulus can be assumed to be about 50% of the bulk matrix [6]. Numerically, the characteristics of the ITZ have been assumed as functions of the aggregate types.

## 3. THE MATHEMATICAL MODEL

In meso scale models, concrete material is treated as a composite material where each component (cement paste, aggregates and ITZ), is considered as a multiphase system where the voids of the skeleton are partly filled with liquid and partly with a gas phase [7, 8]. The liquid phase consists of bound water (or adsorbed water), which is present in the whole range of water contents of the medium, and capillary

water (or free water). The gas phase, i.e. moist air, is a mixture of dry air (non-condensable constituent) and water vapour (condensable gas) and is assumed to behave as an ideal gas.

The approach here is to start from a phenomenological model originally developed by Bažant [9], in which mass diffusion and heat convection-conduction equations are written in terms of relative humidity  $h$ . The coupled system of differential equations for dealing with humidity diffusion and heat transport can be written as:

$$k \frac{\partial h}{\partial t} - \nabla^T \mathbf{C} \nabla h - \frac{\partial h_s}{\partial t} - K \frac{\partial T}{\partial t} + \bar{\alpha} \mathbf{m}^T \frac{\partial \varepsilon}{\partial t} = 0 \quad (1)$$

$$\rho C_q \frac{\partial T}{\partial t} - \nabla^T \mathbf{\Lambda} \nabla T - \frac{\partial Q_h}{\partial t} = 0 \quad (2)$$

where  $k$  is the cotangent of the isotherm slope,  $\mathbf{C}$  is the (relative humidity) diffusivity diagonal matrix,  $dh_s$  the self-densation,  $K$  the hygrothermic coefficient,  $\mathbf{m} = \{1 \ 1 \ 1 \ 0 \ 0 \ 0\}^T$ ,  $\bar{\alpha} = (\frac{\partial h}{\partial \varepsilon_v})|_{T,w}$  equals the change in  $h$  due to unit change of volumetric strain  $\varepsilon_v$  at constant moisture content  $w$  and temperature  $T$ ,  $\rho C_q$  is the thermal capacity,  $\mathbf{\Lambda}$  the thermal conductivity diagonal matrix and  $Q_h$  the outflow of heat per unit volume of solid. The last term in Equation (1) represents the coupling term for connecting hygro-thermal and mechanical responses.

The effective stress, directly responsible for the deformation of the solid skeleton, is addressed for evaluating the mechanical behaviour of each constituent, treated as a porous medium itself. By using the Coleman-Noll method from the entropy inequality, the following relations for the thermodynamic pressure of solid skeleton,  $p_s$ , and effective stress tensor,  $\boldsymbol{\sigma}'$ , can be obtained [10]:

$$p_s = p_w S_w + p_g (1 - S_w) \quad (3)$$

$$\boldsymbol{\sigma}' = \boldsymbol{\sigma} - p \mathbf{I} \quad (4)$$

where

$$p = \begin{cases} p_g - p_{atm}, & \text{if } S \leq S_{ssp} \\ p_g - p_{atm} - (S_w - S_{ssp}) p_c, & \text{if } S > S_{ssp} \end{cases} \quad (5)$$

with  $p_{atm}$  denoting the atmospheric pressure and  $\mathbf{I}$  the second order unit tensor.

From the mechanical viewpoint, the non-local scalar damage model by Mazars has been considered in order to model the damaged behaviour of concrete at both macro and meso level. Hence, the stress-strain relationship in incremental form can be written as:

$$d\boldsymbol{\sigma}' = (1 - d) \mathbf{D} (d\varepsilon - d\varepsilon^T - d\varepsilon^c - d\varepsilon^{sh} - d\varepsilon^0) \quad (6)$$

where  $d$  is the isotropic scalar damage variable,  $\mathbf{D}$  the constitutive matrix,  $d\varepsilon^T$  the strain rate caused by thermo-elastic expansion,  $d\varepsilon^c$  the strain rate accounting for creep,  $d\varepsilon^{sh}$  is due to shrinkage and  $d\varepsilon^0$  represents the autogeneous strain increments (e.g. due to chemical variations) and the irreversible part of the strain rates not contained in the previous terms. By considering the effective stress definition, the macroscopic linear momentum balance equation for the whole medium may be expressed in the form:

$$div(\boldsymbol{\sigma}' + p \mathbf{I}) = [(1 - \phi) \rho_s + \phi S_w \rho_w + \phi (1 - S_w) \rho_g] \mathbf{g} \quad (7)$$

In a meso-scale approach, different hygro-thermo-mechanical characteristics have been accounted for to characterize each concrete phase: cement paste, ITZ and aggregates.

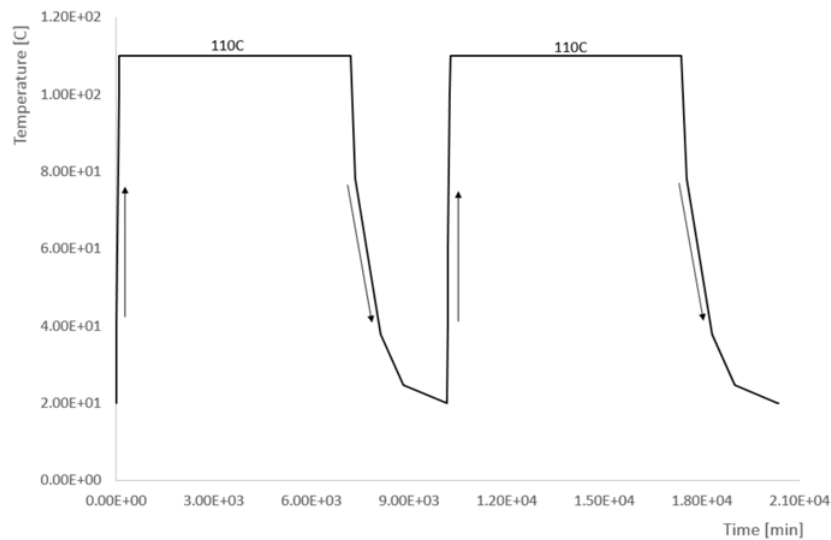


**Figure 2.** Temperature vs. Time.

## 4. NUMERICAL ANALYSES

### 4.1 Models calibration

Numerical models have been calibrated, in terms of hygro-thermal behaviours, referring to the experimental tests carried out by Khoury [11]. These tests considered a slow heating rate ( $1\text{ }^{\circ}\text{C}/\text{min}$ ) for an unloaded sample, starting from  $20\text{ }^{\circ}\text{C}$  (*room temperature*) and reaching a maximum temperature  $T_{\text{max}} = 110\text{ }^{\circ}\text{C}$ . In the tests  $T_{\text{max}}$  has been maintained constant for 5 days and then the sample has been cooled naturally for the subsequent 2 days (see Figure 2).

The sample was in statically determinate conditions and the strain variation was due only to thermal expansion and shrinkage effects. During the heating phase, the internal relative humidity in the sample, initially equal to nearly 100%, decreases and the corresponding strain due to shrinkage triggers. The contraction of the specimen, due to a decrease in humidity, mitigates the thermal expansion. In this first test a mechanical load is not considered and the maximum temperature applied to the sample is sufficiently low so that a possible thermal damage is not activated.

This test has been simulated by adopting two different models as shown in Figure 3, the first one at the macroscale (a classic concrete representation, where the material is seen as an homogeneous one) and the second one at the mesoscale, where concrete has been represented as a three-phase material.

Concrete response in terms of strain vs. time is reported in Figure 4 where the comparison between experimental and numerical results is shown.

It can be noticed that initially, when the thermal load increases, the thermal strain of the sample increases as well (part OA in Figure 4). When temperature reaches its maximum value and remains constant, the total strain decreases (part AB in Figure 4). Such a deformation decrease is due to shrinkage; indeed in this phase relative humidity decreases until reaching room humidity (equal to about 0% at  $110\text{ }^{\circ}\text{C}$ ). This observation is confirmed during the cooling phase in the first thermal cycle and during the thermal reload in the second cycle. The thermal expansion only is recovered during cooling, in fact it can be seen that the strain variation related to OA is equal to BC (cooling phase), and during thermal reloading (part CD). In the second cycle, when temperature is maintained constant, the total strain is also constant, because the sample humidity is zero and, consequently, the total strain corresponds to the thermal one.

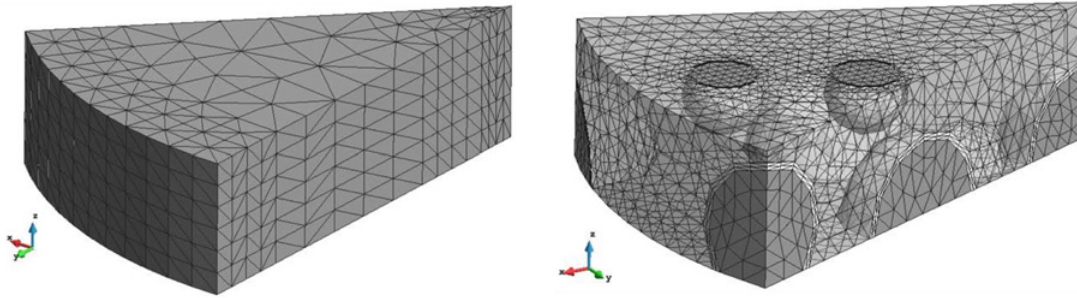


**Figure 3.** Macroscale and Mesoscale Models.

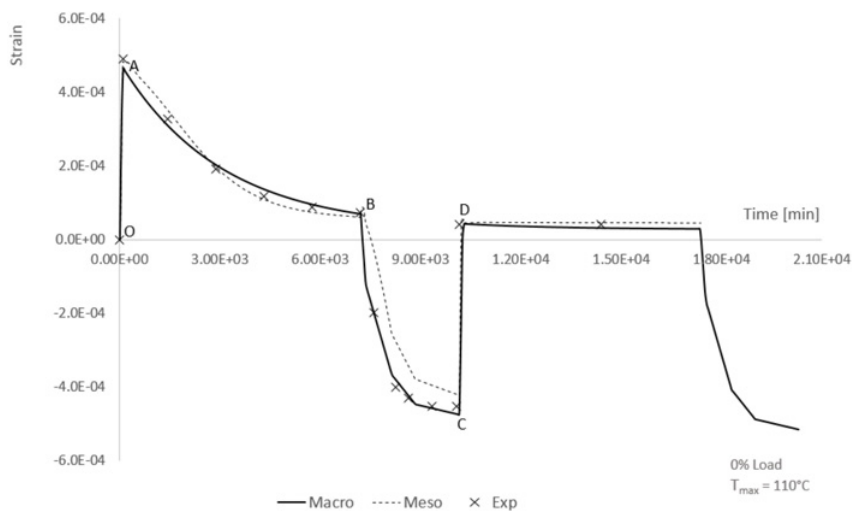


**Figure 4.** Strain vs. Time.

## 4.2 Numerical analyses of concrete at elevated temperatures

After calibration, subsequent numerical investigations have been conducted in order to evaluate the influence of different aggregate types and different thermal loads. Two different aggregate types have been considered: limestone aggregates, whose hygro-thermo-mechanical characteristics were evaluated through calibration and non porous aggregates (basalt aggregates), whose characteristics have been defined from literature.

Initially a slow heating rate has been considered ( $1^{\circ}\text{C}/\text{min}$ ), starting from  $20^{\circ}\text{C}$  and reaching  $300^{\circ}\text{C}$ .

From the first results it is possible to say that, for a slow heating rate, the presence of a porous aggregate considerably improves concrete performances, postponing damage initiation after  $200^{\circ}\text{C}$  (see Figure 5). In this case the same mechanical behaviour has been assumed for the non-porous and porous aggregates.

Subsequently, after the slow heating rate analyses and for the same 3D sample, a heating rate based on the ISO-834 curve reaching  $600^{\circ}\text{C}$  has been accounted for in order to simulate a typical fire. Particularly, the damage evolution for the two different types of aggregate porosities and two

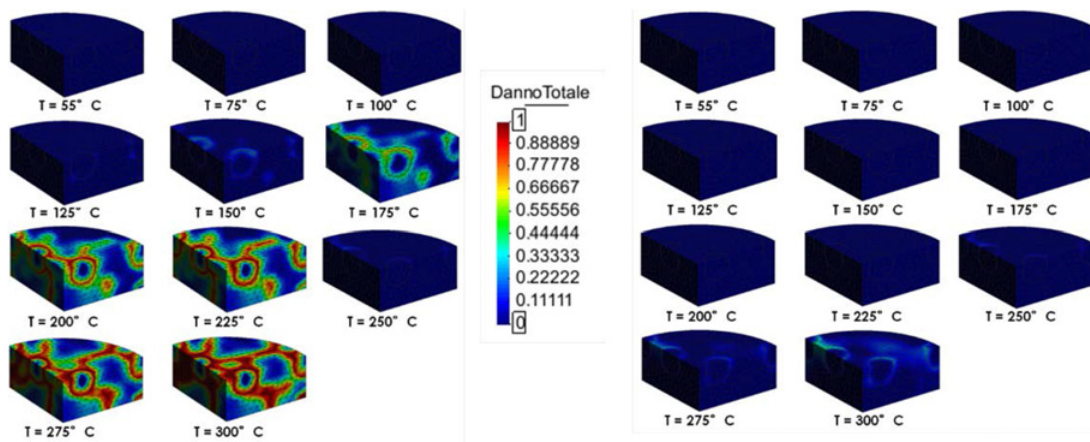


**Figure 5.** Total damage in samples with non-porous (left) and porous (right) grains at different temperatures.

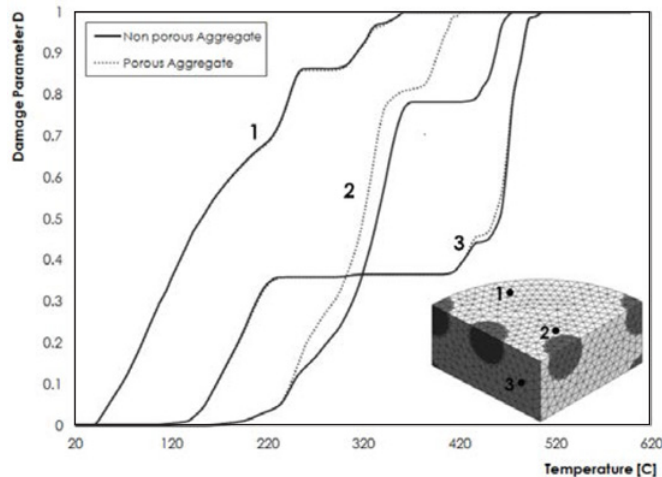


**Figure 6.** Damage evolution under a fast heating rate for porous and non-porous aggregates.

different types of cement paste (a standard and a weaker one, characterized by higher porosity) has been investigated.

By analyzing damage evolution, it can be seen that, for a fast heating rate, different aggregates porosities do not substantially affect the results (Figure 6), as previously seen for slow heating rates; only small damage variations are visible. A delayed effect on damage evolution is instead visible (anyway much smaller than the one obtained under slow heating rates) if we consider a weaker cement paste, i.e. characterized by a higher hydraulic diffusivity (Figure 7).

## 5. CONCLUSIONS

Numerical simulations of homogenous isotropic concrete materials under high temperature conditions, has allowed for obtaining an average evaluation of damage evolution.

To improve damage characterization during the initiation of spalling phenomena, a mesoscale simulation should be performed. At this scale, concrete is represented as a composite material, where

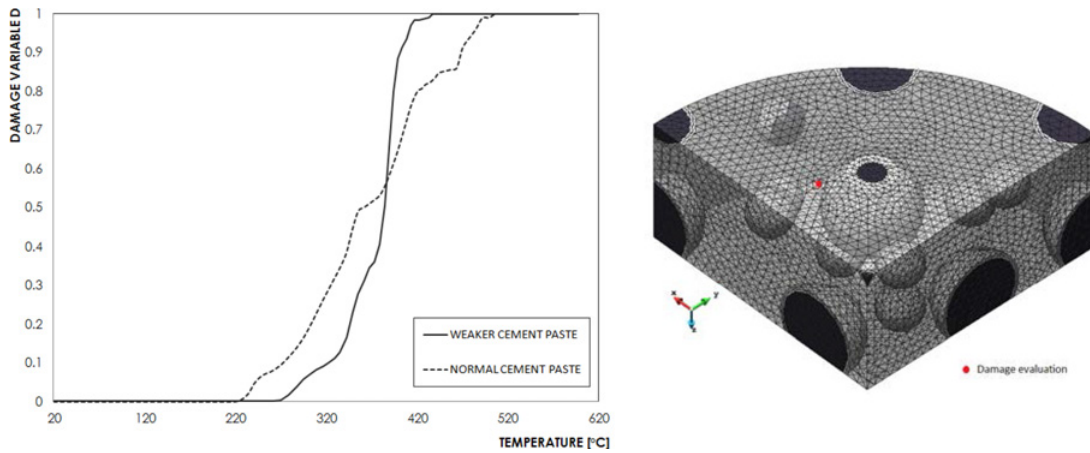


**Figure 7.** Damage evaluation for normal and weaker cement paste during fast heating rates.

each component presents different hygro-thermo-mechanical characteristics that permit to evaluate the internal material hyperstaticity between cement paste and aggregates which increases the internal stress, not visible through macroscale simulations.

The role of aggregates and cement paste porosity has been evaluated by considering 3D numerical models under slow and fast heating rates. It can be hence concluded that during a slow heating rate the presence of porous aggregates improves concrete response instead, when a fast heating rate is accounted for, the aggregate porosity does not substantially influence damage evolution and concrete response depends essentially on cement paste.

## References

- [1] Xotta G., Salomoni V.A. and Majorana C.E., Thermo-hygro-mechanical meso-scale analysis of concrete as a viscoelastic-damaged material, *Engineering Computations*, 30(5), 728–750, 2013.
- [2] Majorana C.E., Salomoni V.A., Mazzucco G. and Khoury G.A., An approach for modelling concrete spalling in finite strains, *Mathematics and Computers in Simulation (Special Issue)*, 80(8), 1694–1712, 2010.
- [3] Bazant Z. and Baweja S., Creep and shrinkage prediction model for analysis and design of concrete structures: Model B3, Adam Neville Symposium: Creep and Shrinkage–Structural Design Effects, ACI SP-194, A. Al-Manaseer Ed., Am. Concrete Institute, Farmington Hills, Michigan, 1–83, 2000.
- [4] Mazars J.A., A description of micro and macroscale damage of concrete structures, *Eng. Frac. Mech.*, 25, 729–737, 1986.
- [5] Scrivener K.L., Crumbie A.K. and Laugesen P., The interfacial transition zone between cement paste and aggregate in concrete, *Interface Science*, 12, 411–421, 2004.
- [6] Hashin Z., Monteiro P.J.M., An inverse method to determine the elastic properties of the interphase between the aggregate and the cement paste, *Cement and Concrete Research*, 32(8), 1291–1300, 2002.
- [7] Gawin D., Majorana C.E. and Schrefler B.A., Numerical analysis of hygro-thermal behaviour and damage of concrete at high temperature, *Mech. Coh. Frict. Mat.*, 4, 37–74, 1999.
- [8] Baggio P., Majorana C.E. and Schrefler B.A., Thermo-hygro-mechanical analysis of concrete, *Int J Num Meth Fluids*, 20, 573–595, 1995.

- [9] Bazant Z.P., Pore pressure, uplift, and failure analysis of concrete dams, Int. Commission on Large Dams, Swansea, UK, 1975.
- [10] Gray W.G., Schrefler B.A., Thermodynamic approach to effective stress in partially saturated porous media, *Eur. J. Mech. A/Solids*, 20(4), 521–538, 2001.
- [11] G.A. Khoury, Strain of heated concrete during two thermal cycles. Part 1: Strain over two cycles, during first heating and at subsequent constant temperature, *Magazine of Concrete Research*, 58(6), 367–385, 2006.